INTEGRATING SEISMIC REFRACTION AND SURFACE WAVE DATA COLLECTION AND INTERPRETATION FOR GEOTECHNICAL SITE CHARACTERIZATION

Michael L. Rucker, P.E.

AMEC Earth & Environmental, Inc., 1405 West Auto Drive
Tempe, Arizona, 85284; michael.rucker@amec.com

ABSTRACT

Recent advances in surface wave measurement capabilities now permit collection of both seismic refraction compressional wave (p-wave) and Rayleigh surface wave (for s-wave) data using the same physical field equipment and geophone arrays. Typical energy sources include sledge hammer for p-wave data and field vehicle, jogging or background ambient noise for refraction microtremor (ReMi) data. Seismograph field sampling rate settings are changed from p-wave to surface wave data collection; the rest of the field setup remains the same. Interpretation of the p-wave and s-wave data sets uses standard procedures. However, results of each data set are used to constrain or verify the results of the other data set. P-wave interpretation proceeds first to interpret interface depths and p-wave velocities in two dimensions across the seismic line profile. The p-wave results provide an initial model for interpreting the s-wave profile from the dispersion curve. Upper or shallow interface depths based on p-wave results are honored, and s-wave velocities for the shallow layers are estimated as about one-half the p-wave velocities. Interpretation of the deeper portion of the s-wave profile based on the dispersion curve then proceeds. The p-wave results provide an effective constraint on the upper portion of the s-wave interpretation to reduce the non-uniqueness of the overall dispersion curve interpretation. At the same time, the s-wave interpretation can be used to identify the absence or presence of a significant velocity reversal condition, and typically provides a considerably greater depth of investigation for the final interpretation. Examples of geotechnical characterization for highway projects in Arizona, Utah and New Mexico using these complementary surface seismic concepts are presented.

INTRODUCTION

Surface seismic methods provide effective shallow subsurface profile characterization for geotechnical engineering applications (see Figure 1). Seismic compressional wave (p-wave) and shear wave (s-wave) velocities are mathematically related to low-strain elastic moduli values, and thus strength in geologic materials. Relatively large volumes of shallow geologic material, typically in layers at scales of several feet vertically and tens of feet laterally, are evaluated. Seismic refraction is an effective tool for horizontal, lateral characterization as well as vertical characterization. The author routinely uses p-wave seismic refraction methods on transportation related projects to characterize geologic material masses for excavation conditions and, in combination with geotechnical borings and test pits, to assist in developing overall site profiles and material characterization for geotechnical design (Rucker, 2000a). Procedures have also been developed to use seismic velocities to assist in developing shrink and swell factors in rock cut and embankment design (Rucker, 2000b). Primary limitations of p-wave seismic refraction are the p-wave propagation assumption of geologic layers or horizons increasing in seismic velocity with depth, profound p-wave response to a water table that limits characterization in saturated horizons, and a need for quiet at sites to properly detect p-wave first arrival signals. The author also uses s-wave seismic methods to assist in assessing geologic material dynamic parameters, typically needed for vibration sensitive foundation design such as at pipeline compressor stations and optical observatories. Prior to the refraction microtremor (ReMi) method becoming available in 2002, s-wave data was typically obtained (Viksne, 1976) using surface refraction with horizontally oriented shear geophones, or by downhole methods using a triaxial geophone array in a geotechnical borehole. Horizontally polarized s-waves were typically generated by striking the ends of a wooden plank coupled to the ground under the wheels of a field vehicle. Rarely, crosshole seismic methods such as Method D-4428 (ASTM, 2000) would be utilized on critical projects. These methods are essential for some applications, such as assessment of Poisson's ratio, because the propagation paths and resulting seismic wave velocities through the subsurface materials for both p-waves and s-waves are consistent and comparable.

Surface wave methods such as spectral analysis of surface waves (SASW) (ASCE, 1998) or refraction microtremor (ReMi) (Louie, 2001), may be used to evaluate s-wave subsurface profiles with velocity reversals, where a lower velocity horizon underlies a higher velocity horizon. The older seismic refraction s-wave method is subject to the same limitations as p-wave seismic refraction, and cannot characterize a velocity reversal, although downhole and crosshole seismic methods can characterize velocity reversals. Similar to the other s-wave methods, surface wave methods are not significantly influenced by a water table since fluids do not transmit s-waves. Unlike the other s-wave methods, surface wave methods can utilize ambient site noise as surface wave energy sources. However, surface wave derived s-wave interpretation results are vertical 1-dimensional profiles, and practical interpretation solutions, especially in complex profiles, are non-unique. Surface waves also result in lower resolution of the model parameters than do refraction compressional waves. Weaknesses in p-wave seismic refraction methods tend to be strengths in surface wave s-wave seismic methods and vice versa. S-wave results can 'see' below a velocity reversal or water table that limits p-wave results. The shallow part of a p-wave profile constrains the non-uniqueness of an s-wave profile, and the 2-dimensional nature of a p-wave profile constrains the limits of a vertical 1-dimensional s-wave profile. At a noisy site, surface wave results provide at least some characterization where p-wave results cannot be obtained. Performing both p-wave and surface wave methods using the same seismic equipment and same geophone array setup provides much more comprehensive shallow subsurface characterization than using either p-wave or surface wave methods alone. Complementary capabilities and limitations of these methods are illustrated in Figure 1.

Figure 1. *Surface seismic characterization of an existing highway rock cut south of Sedona, Arizona as interpreted from a surface seismic line completed along the top of the cut. This seismic line was one of 60 lines completed as part of the geotechnical investigation for design of major improvements and widening of highway State Route (SR) 179 through a mountainous area near Sedona, Arizona. Interpreted p-wave velocities (in feet per second) at various parts of the exposed rock mass are presented in white. The range of p-wave velocities varies laterally across the cut, but p-wave depth of investigation is limited to the high velocity sandstone horizon. S-wave velocities are presented as a 1-dimensional vertical profile. S-wave characterization includes the less competent slope-forming siltstone material underlying the high velocity sandstone, and a very high velocity horizon underlying the slope toe.*

SURFACE SEISMIC MEASUREMENT METHODOLOGIES

Small-scale engineering surface seismic work including surface waves is routinely performed by the author using a standard 12 channel signal enhancement seismograph and a sledgehammer energy source for seismic refraction measurements (Figure 2). Typical objectives for transportation work include rock or cemented soils cut excavation and swell factor characterization, and assisting in bridge foundation and scour assessment. Details of typical seismic refraction field procedures and interpretation methods used to characterize subsurface profiles for transportation investigations are described by Rucker (2000). Refraction microtremor (ReMi) surface wave theory is presented by Louie (2001) and geotechnical field procedures and applications are described by Rucker (2003). Typical depths of investigation for geotechnical characterization vary with geophone array dimensions, available energy sources and subsurface geology. A 120-foot (36 m) geophone array with 10 foot (3 m) geophone spacing and 5 foot (1.5 m) hammer spacing to the nearest geophone for seismic refraction provides sufficient depth of investigation and effective near surface resolution for shallow geotechnical work for depths less than about 30 feet (9 m) for p-waves and often greater than about 60 feet (18 m) for surface waves. This length geophone array is effective with a sledgehammer and can be moved on foot to areas inaccessible by field vehicle such as tops of proposed rock cut areas or incised drainages. When finer shallow detail is needed, the array and hammer spacing is typically halved. Field operations with a two person crew can proceed quickly and efficiently. When terrain or project requirements prevent vehicle access, the equipment can be backpacked to investigation locations. Such mobility makes seismic an effective tool for preliminary subsurface evaluation before drill rig or heavy equipment access must be prepared.

Figure 2. *Field setup for p- and s-wave data collection to assess the subsurface profile for highway SR 179 improvements in Sedona, Arizona along a difficult access sidehill cut and fill using a 12-channel seismograph. A 60 foot (18 m) long 12 geophone array is deployed using a 120 foot (36 m) geophone cable. A 10-lb (4.5 kg) sledgehammer with trigger switch and cable is the p-wave energy source. Traffic on the highway and the operator jogging are ambient s-wave energy sources. Battery, geophones, notebook and other field items are carried by backpack. Drill rig access was not feasible here both due to limited space and the presence of buried utilities in the fill portion of the existing side-hill cut and fill section. Multiple seismic lines were completed end to end to obtain a continuous profile in this area.*

For shallow geotechnical site characterization work, the seismograph needs both fast data sampling rates for compressional wave (p-wave) data (typically 32 to 128 usec), slow data sampling rates for surface wave data for shear wave (s-wave) results (typically 500 to 2,000 usec), and sufficient data memory capability (for example, 16,000 samples per geophone channel). Unless sites have excessive ambient low frequency noise, 4.5 Hz geophones are sufficient for collecting both p-wave and surface wave data. Typical procedures for completing a combination p-wave and surface wave seismic line include the following. Once the equipment (Figure 2) is at the line location, the geophone cable is deployed using a cloth tape if geophone spacing is shorter than the geophone cable takeout spacings. The geophones are placed at the takeout locations and set using the ground spike; a small bubble level is placed on top of the geophones during placement to assure that they are placed vertically (within a half bubble) for proper surface wave data collection. The hammer, strike plate and hammer cable are deployed to the far end of the cable (reverse profile or backshot) and the battery and cabling are attached to the seismograph. Using the sledgehammer energy source, p-wave data sets are collected and printed or stored on disk at the backshot, quarterpoints, center and forward shot locations along the geophone array. An example backshot trace with clear first arrivals is presented in Figure 3. Once the p-wave data has been collected, the seismograph is prepared to collect surface wave data. Unless nearby high voltage power lines require them, filters are typically not used. Channel gains are typically set to 60 db, and for 10 foot (3 m) geophone spacings, the sample rate and sample period are typically set to 1000 microseconds and 12 seconds, respectively. Triggered manually at the seismograph, several (typically four or more) surface wave data sets are collected and stored on disk for later processing. One of the field crew typically jogs alongside the geophone array or jumps just beyond one end of the array to generate fairly repeatable surface wave energy. Interpretation of p-wave and surface wave data will be discussed shortly.
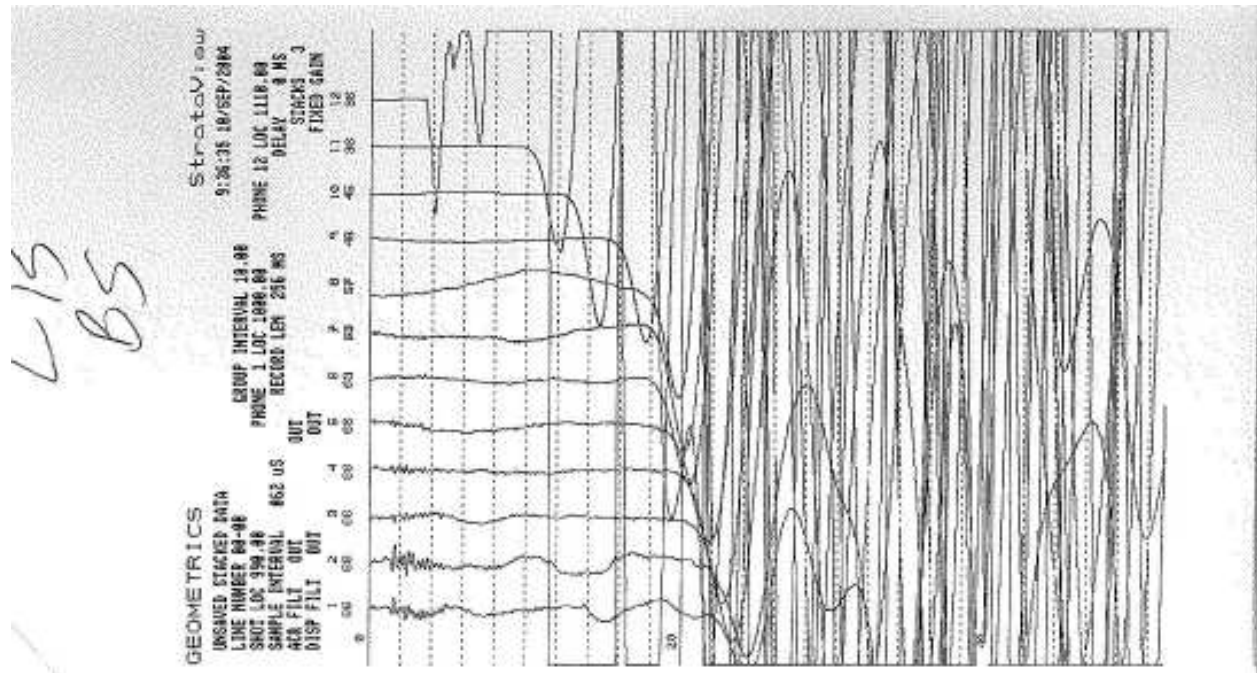
Figure 3. *Example p-wave traces from a seismic line at highway NM 128 near Carlsbad, NM (see also Figures 4 through 7). Geophones were spaced at 10 foot (3 m) intervals, and the sledgehammer shot point was 5 feet (1.5 m) beyond geophone 12. Travel time is indicated in milliseconds along the trace bottom; each vertical dotted gridline is 2 milliseconds. First arrivals are picked manually. The first arrival time at geophone 11 is 10 milliseconds, and the first arrival time at geophone 2 is 22 milliseconds. Signal gains are presented vertically at zero time on the traces. The gains, in decibels, at geophones 12 to 5 are 36, 36, 45, 48, 57, 63 and 63, respectively. Gains at geophones 4 to 1 are 66 db. Based on an initial half-wave time of 2.5 milliseconds at geophone 9, the estimated frequency of first arrival signals propagating along a high velocity refractor indicated by geophones 9 to 1, may be about 200 Hz.*

## INTERPRETATION – EXAMPLE IN EVAPORITE KARST ENVIRONMENT

An example of surface seismic site characterization in an area of evaporite karst at Highway NM 128 near Carlsbad, New Mexico is presented by Rucker and others (2005). Two seismic lines were used to characterize background geologic conditions adjacent to but not in areas of significant collapse (see Figure 4), while fourteen seismic lines were used to characterize the area where karst was impacting the highway. P-wave and s-wave interpretation results for a 'background geologic conditions' line are presented in Figures 5 through 7. Subsurface horizon p-wave velocities and interface depths were interpreted using the intercept time method or ITM (e.g., Mooney, 1973; ASCE, 1998) applied to five shotpoints at array endpoints, center and quarterpoints, along each 12-geophone array. Shallow interfaces with large velocity contrasts were readily interpreted using ITM. By breaking each line into four parts, up to four local p-wave velocities with several variable interface depths can be interpreted laterally along a soil or rock horizon under a shallow surface horizon as shown in Figure 6. In Figure 5, p-wave velocities in the surface horizon ranged from 1,250 to 1,850 feet per second (f/s) (380 to 560 meter per second [m/s]). The first interface interpretation had depths ranging from 1.6 to 4.6 feet (0.5 to 1.4 m). Computed p-wave velocities uncorrected for dip (Figure 5) below the first interface ranged from 3,080 to 6,450 f/s (940 to 1,970 m/s). A deeper, higher velocity horizon was interpreted to begin at depths ranging from 17 to 23 feet (5.2 to 7 m). Computed p-wave velocities uncorrected for dip below the second interface ranged from 10,000 to 13,330 f/s (3,000 to 4,100 m/s).

Figure 4. Highway NM 128 crossing into a typical large-scale depression in a regional setting of sedimentary evaporite rock. Evaporite karst is a geologic hazard that impacts the highway in this general area. Seismic data presented in Figures 3, 5, 6 and 7 were collected in the vicinity.

The interpreted profile in Figure 6 included a soil horizon overlying a rock-like material horizon (upper solid red line, an Aeolian gypsite deposit confirmed by nearby exposure) based on seven individual depth interface points along the subsurface profile at depths of about 1.6 to 4.6 feet (0.5 to 1.4 m). Multiple interpretations of the uncemented surficial horizon velocities resulted in laterally varying p-wave velocities ranging from 1,300 f/s to 1,900 f/s (400 to 580 m/s). The underlying gypsite material horizon had laterally varying p-wave velocities with four interpreted velocities ranging from 3,800 f/s to 5,500 f/s (1,160 to 1,680 m/s). Underlying the gypsite horizon beginning at depths of 17 to 23 feet (5.2 to 7 m), the interpreted p-wave velocity increased to about 10,900 f/s (3,300 m/s). This high p-wave velocity horizon was interpreted to be the top of the Rustler formation which consisted of gypsum and anhydrite.

Recently developed non-linear optimization techniques provide another kind of 'automated' seismic refraction interpretation (Optim, 1999). Performed on p-wave data, modeled seismic velocity changes across a mesh with 2 to 3 foot (0.6 to 0.9 m) typical grid dimensions for 10 foot (3 m) geophone spacings, serves as effective check to an ITM interpretation. However, such an interpretation does not characterize a discrete, shallow interface, often at a depth of 2 to 3 feet (0.6 to 0.9 m), as well as ITM. In calculating ray paths, the non-linear optimization result provides an estimated depth of investigation that can reach deeper than the deepest interface using standard refraction interpretation (Rucker, 2002). In the Figure 6 example, the p-wave depth of investigation was estimated at about 32 feet (9.8 m).
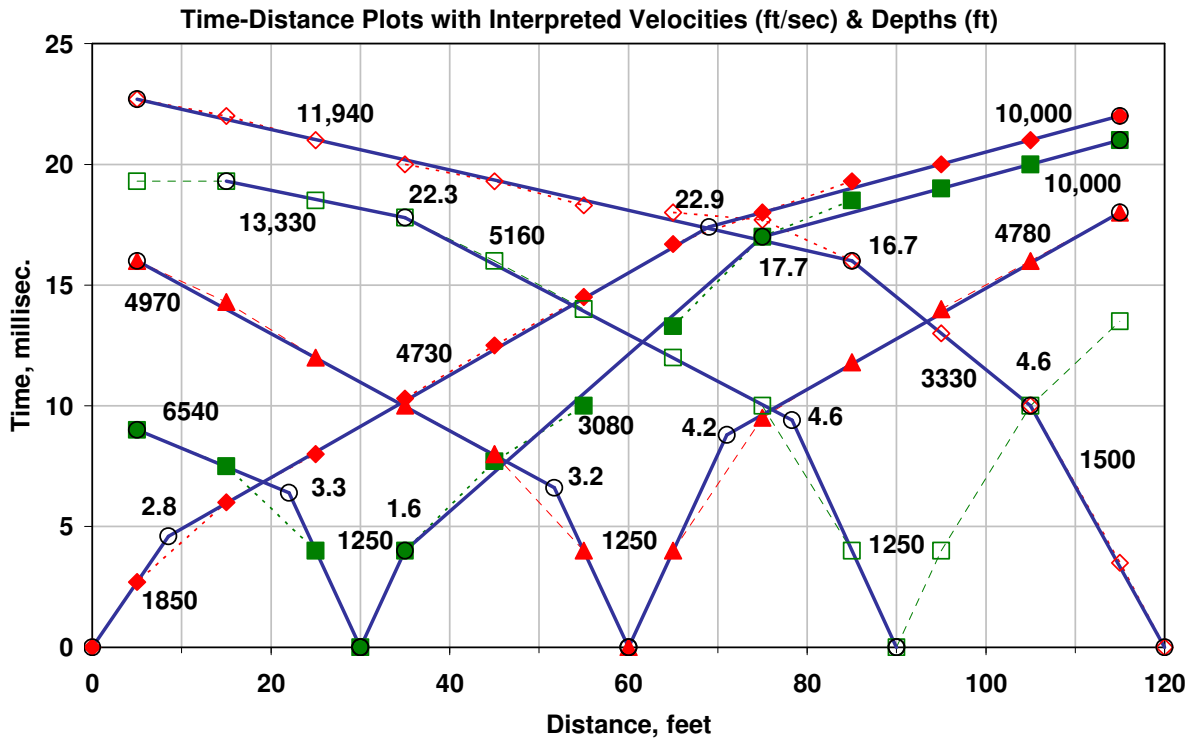
Figure 5. *Example p-wave first arrival time-distance plots used for interpretation in Figure 6. Computed p-wave velocities are labeled in feet per second adjacent to time-distance plot line slopes. Interpreted interface depths in feet are labeled adjacent to changes in slope in the plotted lines. The time-distance plot for the backshot data presented in Figure 3 begins at a time of zero and a distance of 120 feet, and proceeds from right to left along the plot with first arrival times plotted as open diamonds. The various symbols and dashed lines are first arrival point data. The solid lines and open circles represent interpreted model layers velocities and depths based on the first arrival points.*

As described previously, recent surface wave developments, including the refraction microtremor (ReMi) method (Louie, 2001), enable collection and analysis of surface wave data using the same seismograph and field setup (using low frequency 4.5 Hz geophones) used for seismic refraction as described by Rucker (2003). Concurrent p-wave and s-wave interpretations utilize strengths of each method to complement weaknesses of the other. Processing and interpreting ReMi data involves using software (Optim, 2004) to develop a dispersion curve frequency – velocity (or 'slowness;' the inverse of velocity) relationship, and then iteratively building a depth – velocity model that matches the dispersion curve. The color image (Figure 7) presents processed field data as a band of colors trending generally downward from the upper left corner, and data point picks (small open squares) along the lower part of that trend. Data point picks (small open squares) in the color image are dispersion points that form a measured dispersion curve plotted as squares in Figure 7. The s-wave depth – velocity profile presented as a table in Figure 7 corresponds to a best-fit dispersion curve through those dispersion points.
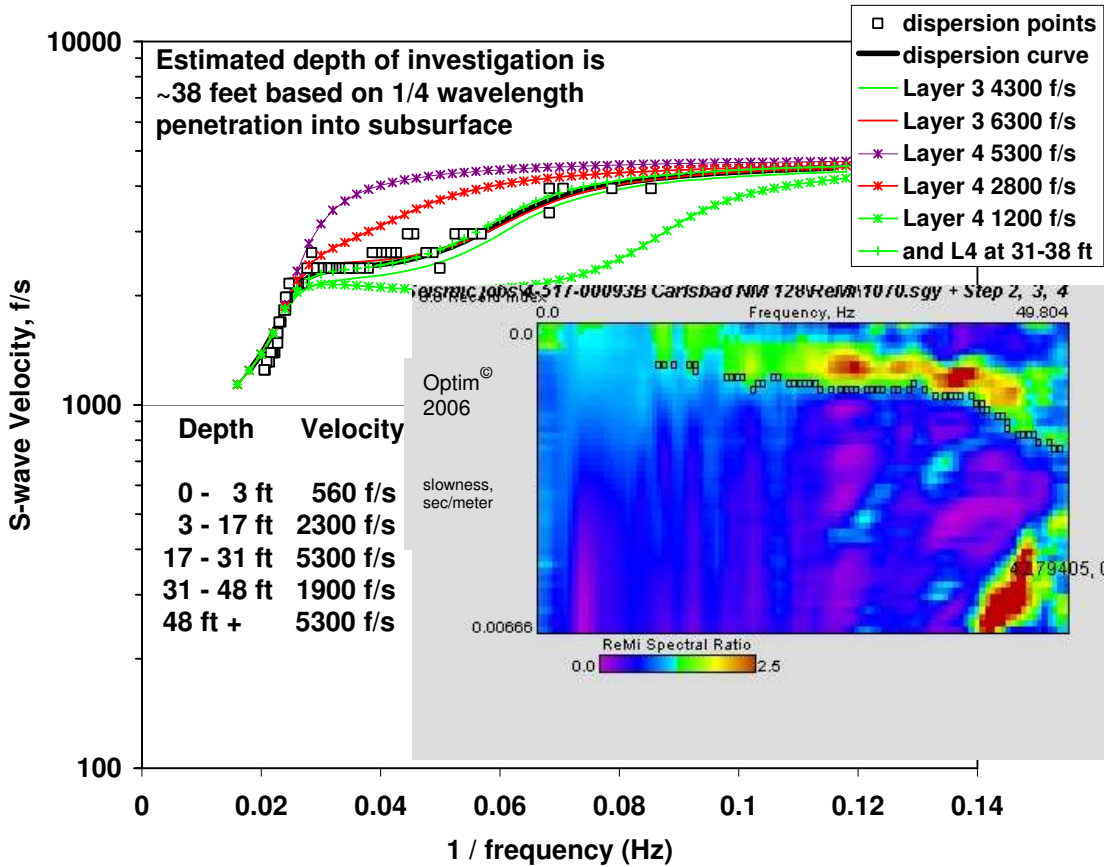
Seismic refraction p-wave interpretations constrain the shallow portion of the s-wave interpretation while the deeper ranging surface wave derived s-wave interpretation can characterize a velocity reversal. An s-wave velocity is typically 0.5 to 0.6 times the corresponding p-wave velocity. The Figure 7 interpretation included constraining the upper three s-wave velocity layers of 560 f/s, 2,300 f/s and 5,300 f/s (170, 700 and 1,620 m/s) to about half the interpreted p-wave velocities in Figure 6. A velocity reversal with s-wave velocity of about 1,900 f/s (580 m/s) was then interpreted to underlie the high velocity horizon at a depth of about 31 to 48 feet (9.4 to 14.6 m). Finally, a high s-wave velocity of 5,300

f/s (1,620 m/s) was interpreted to underlie the subsurface profile. The edge of the large topographic depression shown in Figure 4 formed by ground collapse of roughly 20 feet (6 m) began about 100 meters west of this seismic line. Based on the regional geology and the surface seismic and geotechnical investigation at an evaporite karst site 300 meters west of this seismic line, the 1,900 f/s (580 m/s) s-wave velocity horizon at a depth of roughly 30 to 50 feet (9 to 15 m) was inferred to be especially dissolution-prone, and thus be integral to the development of collapse and karst features along parts of the highway alignment.
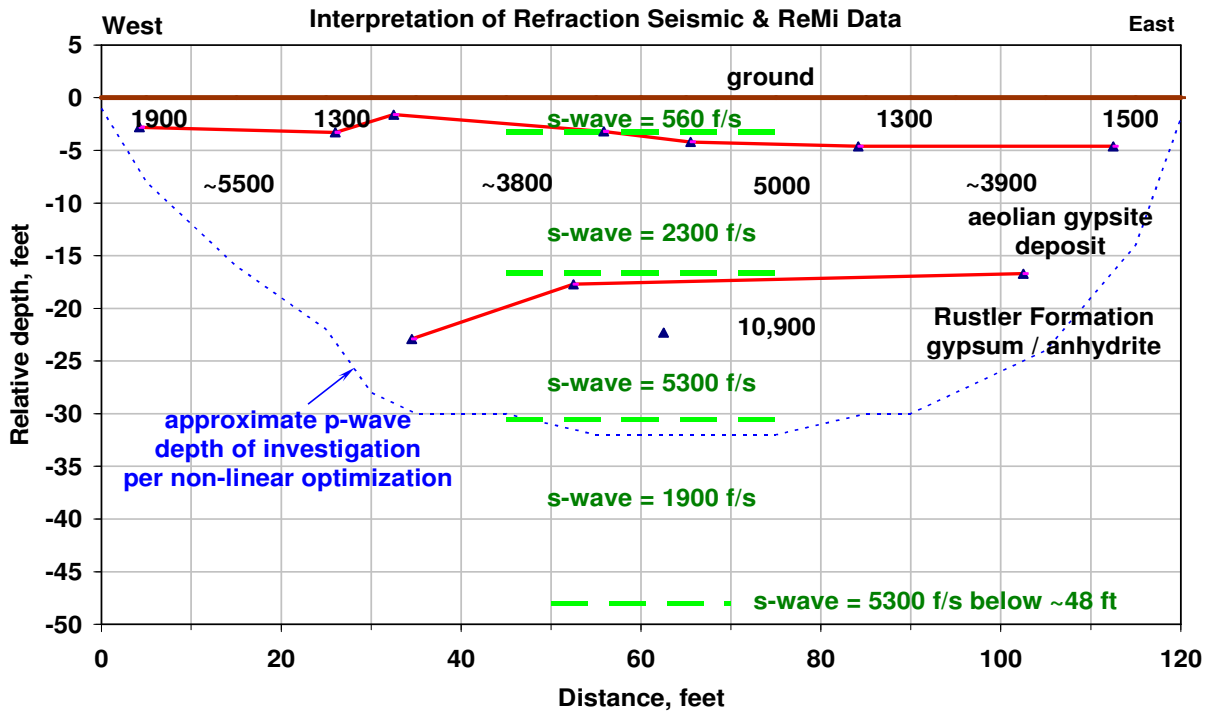
Figure 6. *Example of seismic line interpretations of both 2-dimensional seismic refraction p-wave results (black text in feet per second, solid red lines) based on Figure 5 time-distance plots and 1-dimensional ReMi surface wave (for s-wave velocities) results from Figure 7 (green text, dashed green lines). Results of an interpretation of p-wave depth of investigation are also presented (blue dots). Water table is not a refractor in this profile.*

The effectiveness and limitations in sensitivity and non-uniqueness of dispersion curves to best fit the data is demonstrated in several color plots as alternative dispersion curves shown in Figure 7. At layer 3, the top of the Rustler Formation with p-wave of 10,900 f/s (3,300 m/s) and s-wave 5,300 f/s (1,600 m/s), alternative s-wave velocities of 4,300 f/s (1,300 m/s) and 6,300 f/s (1,900 m/s) are plotted as red and green lines. There is virtually no change in the shape of the dispersion curves and little change in how closely the lines match. If the underlying low velocity Layer 4 is removed (by increasing the s-wave velocity to 5,300 f/s or 1,600 m/s), the purple line with symbols dispersion curve is significantly different from the measured dispersion points; this indicates with confidence that an underlying low-velocity horizon exists deep in the subsurface. Various s-wave velocities for Layer 4, such as 2,800 f/s (850 m/s) (red with symbols) or 1,200 f/s (370 m/s) (green with symbols) significantly changes the shape of the dispersion curve so that effective matching of measured dispersion points and calculated curves by changing s-wave velocity can be made. Finally, reducing the thickness of Layer 4 with a low s-wave velocity of 1,200 f/s or 370 m/s (green line with small pluses) to closely match the measured dispersion points demonstrates the non-unique nature of such interpretations. Even though non-uniqueness may be present in a layer velocity / thickness relationship, the presence or absence of a significant underlying lower velocity horizon can be effectively detected using surface waves.

Figure 7. *Refraction microtremor interpretation for the seismic line presented in Figures 4 through 6. In the ReMi image, the frequency scale from low (0 Hz) to high (49.8 Hz) is left to right, and the s-wave slowness (inverse of velocity) scale low (0.00666 or 150 m/s) to high (0 or infinite m/s) is bottom to top. In addition to the dispersion points and dispersion curve used to obtain depth (in feet) and s-wave velocity (in feet per second) results included in Figure 6, several alternative interpretations are shown to demonstrate aspects of sensitivity and non-uniqueness of interpretation solutions. The shape of the dispersion points and interpreted dispersion curve clearly indicate the presence of a low velocity horizon deep within the profile.*

DEPTH OF INTERPRETATION – A CRITICAL PART OF INTERPRETATION

In the previous section, software based on non-linear optimization was discussed as a means to obtain depths of interpretation of p-wave results. When such software is not available, the deepest interpreted interface depth can be conservatively considered to define a depth of investigation (Rucker, 2002). Since the deepest, highest p-wave velocity horizon extends to an unknown depth, the interpreted depth to the top of that horizon is assumed to be the deepest interpretable point in the seismic refraction profile. An example can be found in Figure 6, where the non-linear optimization based depth of interpretation is about 32 feet (9.8 m), while the depth to the deepest high velocity p-wave interface is only 17 to 23 feet (5.2 to 7 m). The maximum depth of investigation of a seismic refraction array is normally less, and typically much less, than one-third the length of the surface geophone array.

A surface wave derived s-wave depth of investigation can be estimated based on wavelengths in the interpreted frequency – velocity dispersion data. As outlined by Dowding (1996), surface waves penetrate about one-quarter wavelength into the propagating geologic medium. A wavelength is simply calculated as the propagating (s-wave) velocity divided by the wave frequency. An s-wave velocity of 1,000 f/s (300 m/s) at a frequency of 10 Hz has a wavelength of 100 feet (30 m). Further dividing the

wavelength by four yields an estimate of the approximate depth (25 m) to which the propagating wave was influenced. The extent of that influence is the surface wave derived s-wave depth of investigation. An estimate of s-wave depth of investigation is included in the ReMi interpretation summarized in Figure 7. Lower frequency ambient or generated surface energy results in greater s-wave depth of investigation. The surface wave derived s-wave depth of investigation is typically deeper than the p-wave depth of investigation using the same geophone array.

THIN 'CAP ROCK' HORIZON EXAMPLE

Very rapid attenuation of p-wave refraction signals in thin high velocity layers, about 5 to 10 db per wavelength when the layer is less than about one-half wavelength in thickness, has been presented in the literature (O'Brien, 1967; Sherwood, 1967). When a relatively low frequency p-wave first arrival signal propagates through a thin, relatively high p-wave velocity layer, excessive attenuation may not be observed in a relatively short seismic line. In Figure 3, an estimated first arrival signal frequency of about 200 Hz for the 10,900 f/s (3,300 m/s) high velocity layer (Figure 6), results in a wavelength of about 55 feet (17 m). Even though the interpreted 14 foot (4.3 m) thick high velocity layer (based on the surface wave interpretation and concurring estimated p-wave depth of investigation interpretation) is thinner than one-half of the wavelength, the entire seismic line is only about two wavelengths long. Thin-layer attenuation for the case presented in Figure 3 may reduce the signal amplitude by about 10 to 20 db, and the first arrivals can still be effectively obtained across the entire geophone array.
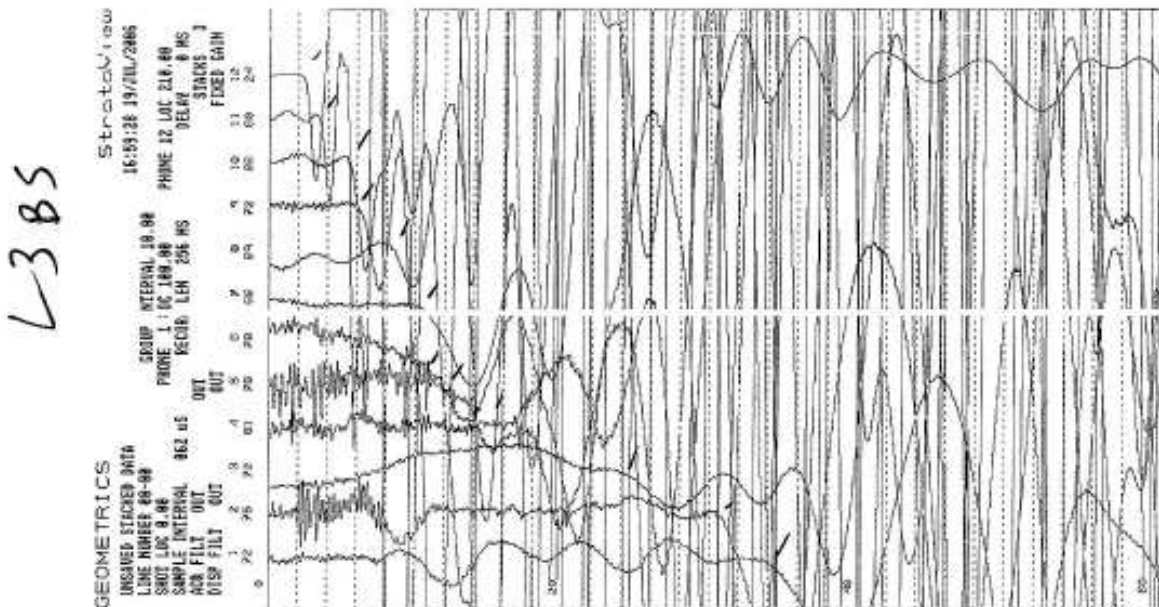

Figure 8. Backshot data at line near St. George, Utah. Trace gains for Geophones 12 to 1 are 24, 60, 66, 72, 69, 66, 78, 78, 81, 72, 75 and 72 db, respectively. Manual field picks of first arrivals are marked on the printout. A thin high velocity layer is indicated by first arrival signals at geophones 12 through 4. An estimated first arrival frequency at geophones 12 through 9, based on an initial half-wave time of about 1.5 msec., may be about 333 Hz. The p-wave velocity in this layer is interpreted in Figures 9 and 10 to be about 5,000 f/s (1,500 m/s). The resulting wavelength is about 15 feet (4.6 m), which is greater than twice the estimated thickness of the high velocity layer through most of the line. Thin-layer attenuation may be anticipated to reduce the signal amplitude by about 20 to 60 db across the line depending on further frequency or other propagation or discontinuity effects. At geophones 3 to 1, the thin layer first arrival is missing.

Thin horizons of harder sedimentary rock, typically limestone, within thicker soft formations, typically claystone, are common through a proposed new highway alignment south of St. George near the Arizona border in southwest Utah. Five seismic lines were completed at selected locations along this alignment, primarily to characterize proposed highway cuts. Groundwater was not present within the p-wave depth of investigation. Data and interpretations presented in Figures 8 through 11 of one of those lines clearly demonstrate limits of the p-wave and surface wave derived s-wave methods individually, and the strengths of using both p-wave and s-wave data together to synthesize an overall understanding of the subsurface significantly improved to the individual interpretations.
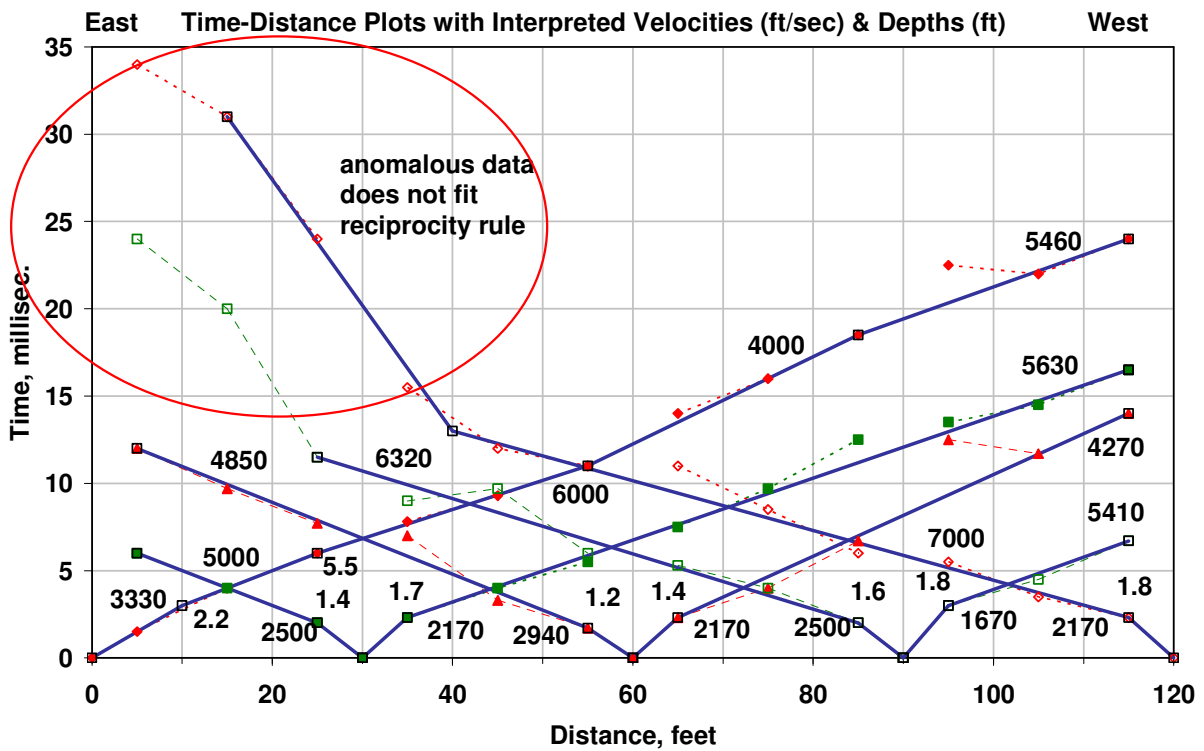
Figure 9. *P-wave first arrival time-distance plots in shallow, thin high velocity layer environment at Atkinville, Utah (near St. George, Utah). Computed p-wave velocities and interface depths are labeled similar to plots in Figure 4. Red and green points and associated dashed lines are first arrival picks and trends in the various directions from source locations. The reciprocity rule that total travel times in the forward and reverse directions must be equal for valid seismic refraction analysis is not satisfied for some data. Anomalous seismic data is circled; possible reasons for the anomalies include excessive attenuation of first arrival signals (see Figure 8) in a thin high velocity horizon. That horizon becomes thicker along the west half of the seismic line as presented in Figure 10. Alternatively, significant fracturing in the high velocity horizon prevents effective p-wave transmission through the high velocity horizon Reciprocity in forward and reverse directions is maintained for shorter subsets of the time-distance plots.*

An example set of geophone data traces with attenuation characteristic of a thin layer are presented in Figure 8, and seismic refraction time-distance plots at the seismic line are presented in Figure 9. Shorter portions of the time-distance plots allowed effective interpretations of the first subsurface interface and underlying higher p-wave velocities. Interpretations are presented in Figure 10. Longer portions of the time-distance plots include data anomalies that prevent effective interpretation of the longer time-distance plots. Greater attenuation of first arrival signals in a thin high velocity layer may account for

these anomalies; the anomalies are not present in the western part of the seismic profile where the thin high velocity layer is interpreted to have a greater thickness. Surficial horizon p-wave velocities are interpreted to be 2,000 to 3,300 f/s (610 to 1,000 m/s) to depths of about 1 to 2 feet (0.3 to 0.6 m). The underlying high velocity horizon has p-wave velocities of 5,000 to 6,100 f/s (1,520 to 1,860 m/s). Based on excavatability in cemented geological materials presented by Rucker and Fergason (2006), excavation refusal at depths greater than about 1 to 2 feet (0.3 to 0.6 m) could be anticipated using backhoes or trackhoes with hydraulic horsepower less than about 250 hp (194 KW) at this seismic line. A Case 580M backhoe (76 hp, 61 KW) encountered refusal at a depth of 1.5 feet (0.5 m) in a test pit at this location. Over the east half of the seismic line, the interpreted p-wave depth of investigation was only about 3 feet (0.9 m); it extended down to about 12 feet (3.7 m) at the west end of the seismic line.
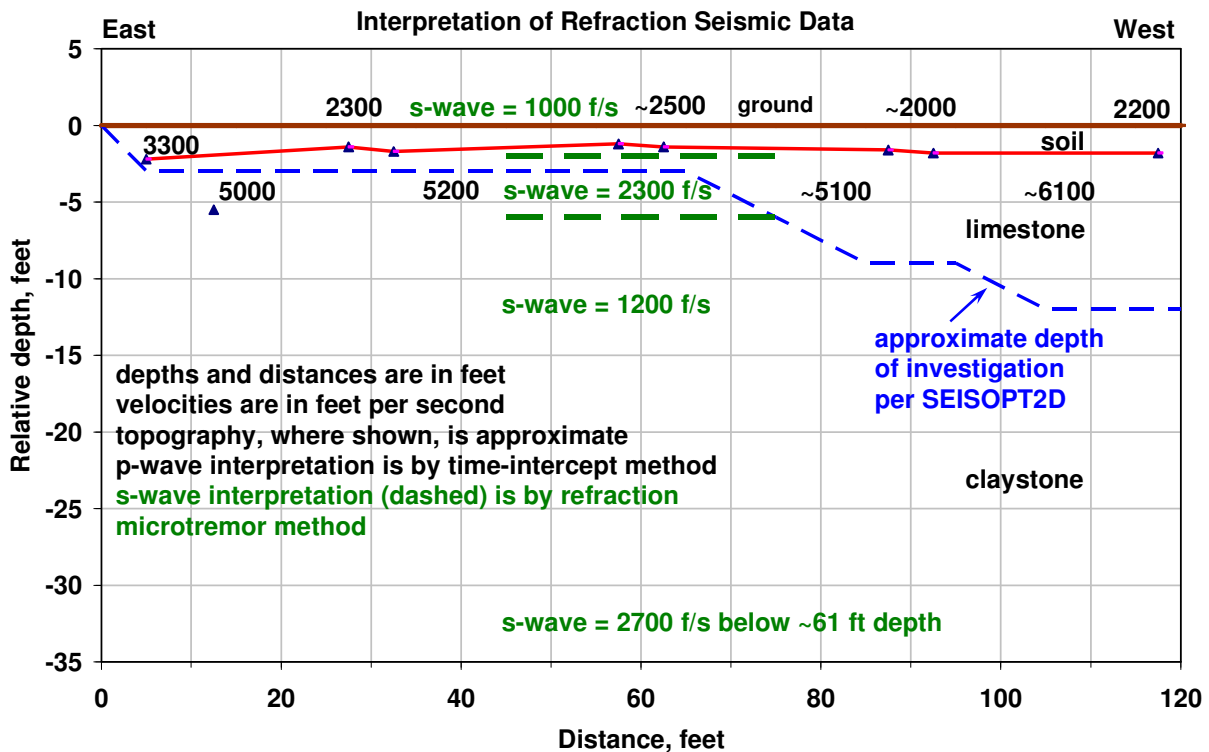
Figure 10. *Seismic line with seismic refraction 2-dimensional interpretation (black text, red lines) of top of shallow high velocity rock-like material across the seismic line and 1-dimensional ReMi s-wave profile showing underlying deep lower velocity material (green text, green dashed lines). P-wave interpretation by non-linear optimization (blue dots) verifies the very shallow p-wave depth of investigation.*

Characteristics of the subsurface deeper than 3 feet (0.9 m) at this line are evident in the ReMi surface wave results and interpretations presented in Figures 10 and 11. Using the p-wave seismic refraction results to constrain a surface horizon s-wave velocity, depth to first interface, and shallow rock-like material horizon s-wave velocity, the vertical s-wave profile presented in Figures 10 and 11 was interpreted. The ReMi interpretation was predominantly influenced by the deeper low velocity horizon; ReMi alone would not be expected to effectively detect the thin high velocity layer. Thus, neither seismic method alone, p-wave seismic refraction, or surface wave refraction microtremor, could effectively characterize the subsurface profile to a depth of even 10 feet (the 3 m). Used together, however, potential excavation issues in the competent shallow high velocity horizon characterized by p-wave seismic refraction and soft underlying (and possibly very erodable) material characterized by surface

wave ReMi that could be exposed in a highway rock cut were effectively addressed in the surface seismic results.
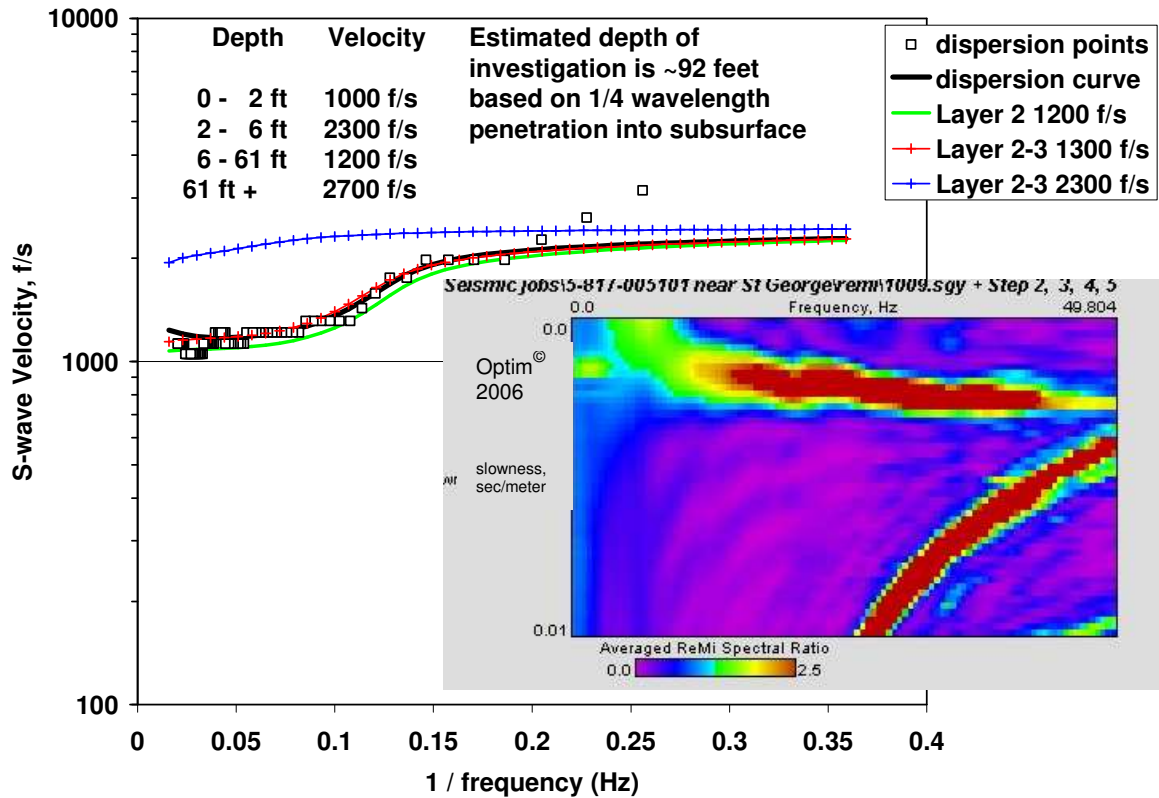

Figure 11. *ReMi s-wave interpretation and profile for seismic line with a shallow, thin rock-like material horizon. Dispersion points were selected along the lower boundary of green and blue in the frequency – slowness (1/velocity) image in the figure. Ignoring the shallow, thin high velocity layer had very little impact on interpreted alternate dispersion curves (red and green lines). A dispersion curve for a uniform high velocity rock-like material of 2,300 f/s (700 m/s) extending from 2 to 61 feet or 0.6 to 18 m (blue line) that was dissimilar to the dispersion points verified the interpretation of deep lower velocity materials in the subsurface profile.*

UTILITY TRENCH EXCAVATION STABILITY HAZARD EXAMPLE

Utility trench excavation is commonly performed in roads and streets, and can present collapse hazards that threaten workers, bystanders and adjacent buried and surface facilities. Geotechnical investigations for buried utilities typically include test borings at prescribed distances to depths below the deepest planned excavation to characterize subsurface excavation and stability conditions. Figure 12 presents surface seismic results on a planned storm sewer alignment where a boring could not be advanced to the necessary planned depth of 10 feet (3 m). The alignment was in an alluvial fan floodplain near an ephemeral drainage in the vicinity of a small volcanic mountain that was a potential source for cobbles and boulders in the alluvium. Relict buried drainage channels consisting of cohesionless sands and gravels could be expected in the alluvium. Refusal of the hollow stem auger at a depth of 4 feet (1.2 m) in the borehole was probably due to the presence of cobbles and boulders. Groundwater was not encountered in project borings that were to advanced to the proposed depths for project design.

Seismic refraction p-wave velocities of 3,600 to 4,800 f/s (1,100 to 1,460 m/s) were consistent with the presence of a horizon of dense to very dense clayey cobbles and boulders (Rucker, 2004) beginning at depths of about 2 to 6 feet (0.6 to 1.8 m) at the seismic line. Large trackhoe or equivalent excavation equipment with power greater than 250 hp (186 KW) would typically be needed to excavate in these materials. Once excavated, trench walls in such materials typically behave as stable ground with normal shoring for construction safety. ReMi interpretation was constrained by the p-wave profile for the upper two layers, resulting in an s-wave velocity profile of 650 f/s (200 m/s) at 0 to 4 feet (0 to 1.2 m) depth and 1,900 f/s (580 m/s) below 4 feet (1.2 m) in depth. The ReMi results also interpreted the presence of a lower s-wave velocity horizon of 1,100 f/s (335 m/s) between depths of about 15 to 36 feet (4.6 to 11 m). In this geologic setting, an s-wave velocity of 1,100 f/s (335 m/s), consistent with a p-wave velocity of about 2,000 to 2,200 f/s (610 to 670 m/s), is typically indicative of a cohesionless granular soil such as a gravelly sand or sandy gravel. Once excavated, trench walls in such cohesionless granular materials may continue to ravel, run and behave as unstable ground requiring extensive shoring or other stability procedures to maintain trench integrity. Excavation in this portion of the project alignment was not anticipated to extend to a depth where a significant zone of potentially unstable cohesionless materials might be encountered.
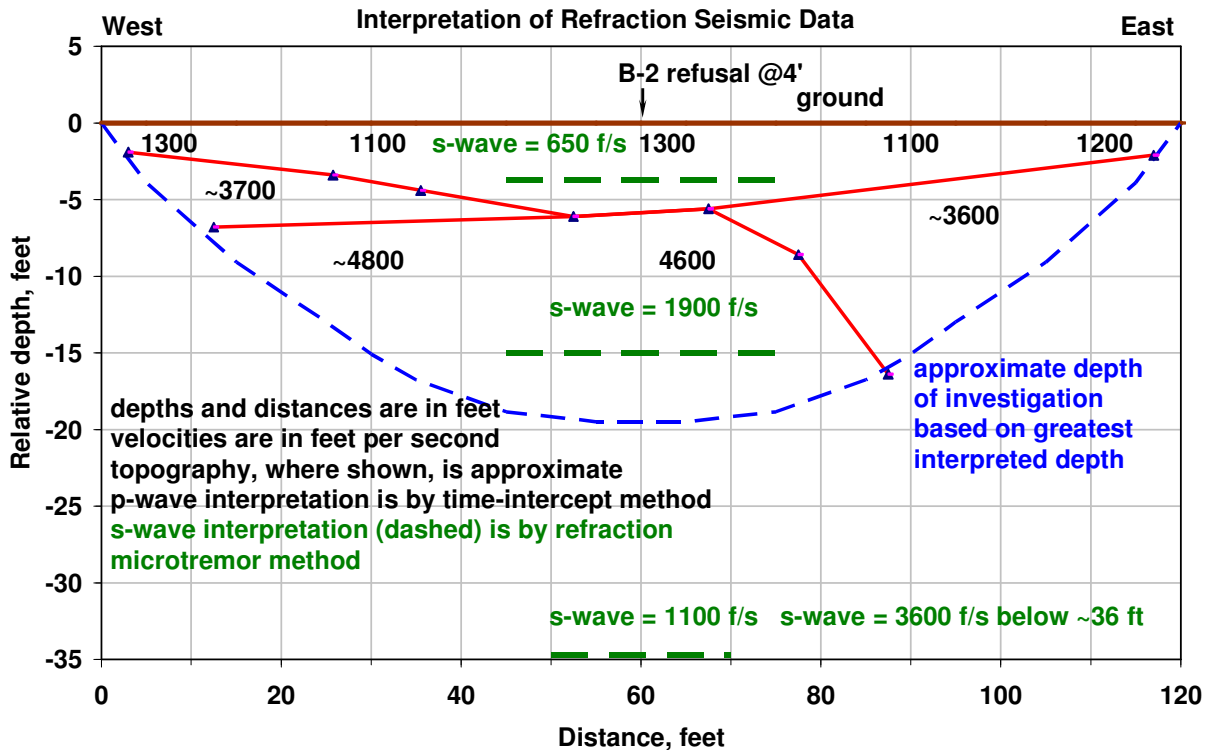
Figure 12. *Results of seismic line on proposed storm sewer alignment where geotechnical boring encountered shallow refusal. Higher p-wave velocities are consistent with clayey cobbley ground where boring refusal could be anticipated. The s-wave profile includes a lower velocity zone at depth between 15 to 36 feet (4.6 to 11 m) that is consistent with cohesionless sands and gravels in this geologic setting.*

SUMMARY

Shallow surface seismic capabilities including both p-wave seismic refraction and surface wave based s-wave vertical profiling by ReMi or other means provides significantly improved subsurface

characterization compared to either p-wave or surface wave results alone. Unlike other s-wave methods, seismic refraction and ReMi data can be collected in the field using a single equipment setup without constraints of special energy sources or source setups. Velocity reversal conditions can be detected and characterized using the combination of p-wave and surface wave results. Combined p-wave and surface wave results can contribute significant insight into the characterization of subsurface profile geometries and, through seismic velocities, material strengths. However, positive identification of subsurface lithologies and confirmation of interpreted results requires information and knowledge from other geotechnical / geologic exploration such as borings, test pits and geologic mapping. Scales of sampling using surface seismic methods must be kept in mind when applying results to characterization and design. Successful execution of surface seismic work requires skilled and experienced personnel in both field work and interpretation; this is perhaps the greatest limitation to the successful application of these methods to geotechnical engineering. As experience develops using both refraction (p-wave) and dispersion (surface wave) physics in a combined field and analysis operation, geotechnical engineering characterization should benefit from the application and contribution of surface seismic methods.

REFERENCES

American Society of Civil Engineers (ASCE), 1998, Geophysical Exploration for Engineering and Environmental Investigations, Technical Engineering and Design Guides as Adapted from the US Army Corps of Engineers Manual (EM 1110-1-1802), No. 23, ASCE Press, Reston, VA, 7-23.

American Society for Testing and Materials (ASTM), 2000, Annual Book of ASTM Standards, Volumes 04.08 Soil and Rock (I) & 04.08 Soil and Rock (II), ASTM, West Conshohocken, PA.

Dowding, C.H., 1996, Construction Vibrations, Prentice-Hall, Inc.

Louie, J.L., 2001, Faster, Better, Shear-wave velocity to 100 meters depth from refraction microtremor arrays; Bulletin of the Seismological Society of America, **91**, 347-364.

Mooney, H.M., 1973, Engineering Seismology Using Refraction Methods, Bison Instruments, Inc., Minneapolis, Minnesota.

O'Brien, P.N.S., 1967, The use of amplitudes in seismic refraction survey, in Musgrave, A.W. (ed), Seismic Refraction Prospecting, Society of Exploration Geophysicists, Tulsa, Oklahoma, 85-118.

Optim, L.L.C., 1999, SeisOpt2D Version 1.0 software package by Optim, L.L.C., of Reno, Nevada.

-------------------2004, ReMi Version 3.0 software package: Optim Software and Data Solutions, UNR-MS-174, 1664 N. Virginia St., Reno, Nevada, 89557.

Rucker, M.L. 2000a, Applying the seismic refraction technique to exploration for transportation facilities; 1st International Conference on the Application of Geophysical Methodologies to Transportation Facilities and Infrastructure, St. Louis, Missouri, FHWA, December 11-15.

------------------2000b, Earthwork factors in weathered granites by geophysics, in Nazarian, S. and Diehl, J. (eds), Geotechnical Special Publication No. 108: ASCE, Reston, Virginia, 201-214.

------------------2002, Seismic refraction interpretation with velocity gradient and depth of investigation, 2nd International Conference on the Application of Geophysical and NDT Methodologies to Transportation Facilities and Infrastructure, Los Angeles, California, FHWA, April 15-19.

------------------2003, Applying the refraction microtremor (ReMi) shear wave technique to geotechnical engineering; 3rd International Conference on the Application of Geophysical Methodologies to Transportation Facilities and Infrastructure, Orlando, Florida, FHWA, December 8-12.

------------------2004, Percolation theory approach to quantify geo-material density-modulus relationships, 9th ASCE Specialty Conf. on Probabilistic Mechanics and Structural Reliability, Albuquerque, New Mexico, July 26-28.

Rucker, M.L., G. Crumb, R. Meyers and J.C. Lommler, 2005, Geophysical identification of evaporite dissolution structures beneath a highway alignment, *in* Beck, B.F., Sinkholes and the Engineering and Environmental Impacts of Karst: Geotechnical Special Publication No. 144, ASCE, Reston, Virginia, 659-666.

Rucker, M.L. and Fergason, K.C., 2006, Characterizing unsaturated cemented soil profiles for strength, excavatability and erodability using surface seismic methods, *in* Miller, G.A., Zapata, C.E. Houston, S.L. and D.G. Fredlund, Unsaturated Soils 2006, Geotechnical Special Publication No. 147: ASCE, Reston, Virginia, 589-600.

Sherwood, J.W.C., 1967, Refraction along an embedded high-speed layer, *in* Musgrave, A.W. (ed), Seismic Refraction Prospecting, Society of Exploration Geophysicists, Tulsa, Oklahoma, 138-151.

Viksne, A., 1976, Evaluation of In Situ Shear Wave Velocity Measurement Techniques, REC-ERC-76-6, Division of Design, Engineering and Research Center, U.S. Department of the Interior, Bureau of Reclamation, Denver, Colorado.